Title:

Spatial and temporal control of expression with light-gated LOV-LexA

Authors:

Inês M.A. Ribeiro*, Wolfgang Eßbauer, Romina Kutlesa, and Alexander Borst

Max Planck Institute of Neurobiology

Am Klopfersptiz 18, 82152 Martinsried, Germany

* corresponding author, ribeiroinesma@gmail.com

Abstract:

The ability to drive expression of exogenous genes in different tissues and cell types, under control of specific enhancers, has catapulted discovery in biology. While many enhancers drive expression broadly, several genetic tricks have been developed to obtain access to isolated cell types. However, studies of topographically organized neuropiles, such as the optic lobe in fruit flies, have raised the need for a system that can access subsets of cells within a single neuron type, a feat currently dependent on stochastic flip-out methods. To access the same subsets of cells consistently across flies, we developed LOV-LexA, a light-gated expression system based on the bacterial LexA transcription factor and the plant-derived LOV photosensitive domain. Expression of LOV-Lex in larval fat body as well as pupal and adult neurons enables spatial and temporal control of expression of transgenes under LexAop sequences with blue light. The LOV-LexA tool thus provides another layer of intersectional genetics, allowing for light-controlled genetic access to the same subsets of cells within an expression pattern across individual flies.

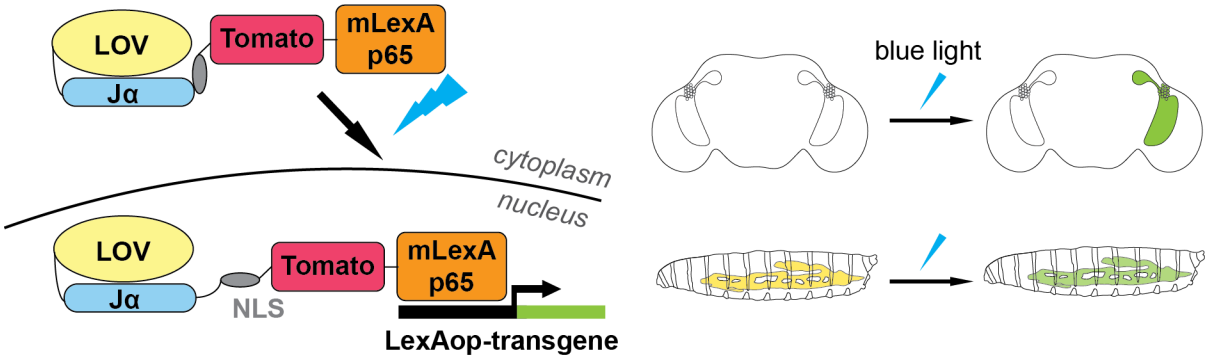

Introduction:

Patterned expression of genes is essential for differentiation of distinct cell types. Enhancers defining expression patterns have long been used to control binary expression systems, that provide genetic access to multiple single cell types to study their development and function. Binary expression systems couple enhancer-led expression of an exogenous transcription factor to expression of a transgene, that sits downstream of promoter sequences exclusively bound by the exogenous transcription factor. The GAL4-UAS system uses the yeast transcription factor GAL4 under control of an enhancer [1]. Random insertions of P-elements into the genome were used to obtain enhancers [2-9]. More recently, stretches of noncoding genomic DNA carved out of known gene enhancers, or from prediction of enhancers at a global scale, have been extensively used to generate large collections of driver lines [10-14]. In addition, other binary expression systems were introduced. The LexA-LexAop [15] and the QF-QUAS [16, 17] both rely on exogenous transcription factors and DNA binding sequences and can be combined with GAL4-UAS, allowing for independent genetic access to multiple single cell types in the same organism [18-20, 21, for eg.]. The spatial resolution, or cell type-specificity of binary expression systems, is determined by the enhancer driving expression of the exogenous transcription factor. Given that it is still not possible to design enhancers specific for many cell types [22], it is necessary to screen for expression patterns of interest to obtain enhancers for the cell type of interest.

Several methods, under the umbrella of intersectional genetics, were developed to further restrict transgene expression in binary expression systems. The globular nature of the GAL4 activation and DNA-binding domains enables separation of GAL4 into two parts, with each split-GAL4 half placed under the control of a different enhancer [23]. The final transgene expression occurs only in cells that express both split-GAL4 halves. Existing collections of split-GAL4 lines targeting single neuron types were established by screening for enhancer pairs that together provide exclusive access to specific cell types of interest [21, 24-42]. Another powerful method of restricting expression to single or fewer cells is stochastic labeling based on the FLP/FRT system, originally derived from yeast [43]. The recombinase flipase (FLP) placed under control of a heat shock promoter, is expressed after a period of heat shock at 37ºC (from the rearing temperature of 25ºC for fruit flies) and binds its target sequence FRT to recombine the sequences between two FRT sites [44, 45]. There are many FRT sites inserted along *Drosophila* chromosomes that allow for recombination of chromosome arms carrying specific gene mutations or knock-ins [45-47], and the creation of cell clones genetically different from surrounding cells [45]. Insertion of FRT sites flanking a STOP cassette that precedes a transgene makes it possible to ‘flip in’ or ‘flip out’ the STOP cassette and either prevent or facilitate expression of the transgene in a stochastic manner [45, 48, 49]. Despite providing specific expression to single cell types, these methods require extensive screening, with an average success rate lower than ten percent [for eg., 20, 39, 50].

Intersectional genetics also includes several methods to limit expression temporally. Temperature sensitive mutations in Gal80 (Gal80ts) [51], a protein that binds and inhibits transcriptional activity by GAL4 [52], has been extensively employed to add experimenter-controlled temporal resolution.

Flies are transferred from 18ºC, at which temperature Gal80ts is fully functional leading to inhibition of transcription by GAL4, to 29ºC at which Gal80ts is no longer functional, and GAL4 is free to drive transcription [51]. Both heat shock promoter driving FLP/FRT systems and Gal80ts can be combined with the UAS-GAL4, adding temporal control and, in the case of FLP/FRT system, spatial control, albeit stochastic, to the expression pattern of a particular enhancer regulating expression of GAL4 [53]. In addition to providing temporal and spatial control however, heat shock at 37ºC or longer periods of incubation at 29ºC also unleash a stress response in all cells of the organism that may affect experimental outcomes. Temporal control of initiation of expression has also been achieved with use of transcription factors modified to drive transcription only in the presence of an ingestible drug [54]. Drugs can have off-target effects that may also alter experimental outcomes. In addition, none of these systems imposes consistent spatial restriction to the expression pattern created by the enhancer upstream GAL4.

With several recent advances in optics and laser technology, light is now easily modulated at the level of its spectrum, intensity and even shape [55]. The high spatial and temporal precision of light pulse delivery to living organisms has the potential to take the spatial and temporal resolution of transgene expression to new levels. Several photosensitive proteins have been introduced into exogenous systems to amass the advantages of light as a precise trigger [56, 57]. Phytochromes (Phy) are sensitive to red and far-red light when bound to the phycocyanobilin (PCB) chromophore, and translocate to the nucleus in presence of light to bind the phytochrome interacting factor (PIF) [58]. In the Photo-GAL4 expression system, the PhyB and PIF were added to each split-GAL4 half instead of the zinc finger, turning the reconstitution of a complete GAL4 dependent on red light [59]. To function however, Photo-GAL4 requires addition of the PCB, a chromophore that is absent in animal cells but essential for photosensitivity of PhyB [58], limiting Photo-GAL4 to use in *ex vivo* experiments [59]. The cryptochrome split-LexA system similarly draws on insertion of cryptochrome 2 (CRY2) and its binding partner, the cryptochrome interacting protein (CIB), into the LexA DNA binding domain and the transactivator domain, to gate reformation of the full LexA-transactivator with blue light [60, 61]. Cryptochromes are central to circadian rhythm in animals and bind to flavin adenine dinucleotide for photosensitivity, a chromophore that exists naturally in animal cells. However, the cryptochrome split-LexA system is leaky in the absence of light delivery (data not shown).

To circumvent these limitations and expand the photosensitive toolbox in *Drosophila*, we developed a light-gated expression system based on the light, oxygen or voltage (LOV) domain originally found in oat phototropin 1 (*Atena sativa*) [62-64] and LexA [65-68]. Here, we show that LOV-LexA gates expression of transgenes with blue light *in vivo*, in several cell types in larval, pupal and adult fruit flies. LOV-LexA thus adds another layer of spatiotemporal control to expression of transgenes in *Drosophila* that is combinable with existent binary expression systems, and transferable to other model organisms.

Results:

Design of an expression system gated by light

The second LOV2 domain of *Atena sativa* phototropin 1, AsLOV2, is photosensitive [69-72]. Exposure to blue light causes the Jα helix to undock and unfold, freeing its C-terminus [69]. This property arises from interactions with flavin, the blue light-absorbing chromophore present in animal cells, and can be used to expose a small peptide of up to 10 amino-acid residues that is added to or integrated into the Jα C-terminus [62, 63, 69, 73, 74]. This photosensitive system has been used to cage several peptides in diverse genetic tools, including the nuclear localizing signal (NLS) to shuttle proteins to the nucleus, an integrator of neuronal activity and reporters of protein-protein interactions [75-91]. Recent work employed directed evolution on the native AsLOV2 to develop the evolved LOV (eLOV), that presents improved stability in the dark state due to three single nucleotide mutations [86]. We selected the eLOV domain and fused it to the short NLS from SV40 [92], to make eLOVnls, and regulate availability of the NLS to the cell milieu with blue light [77].

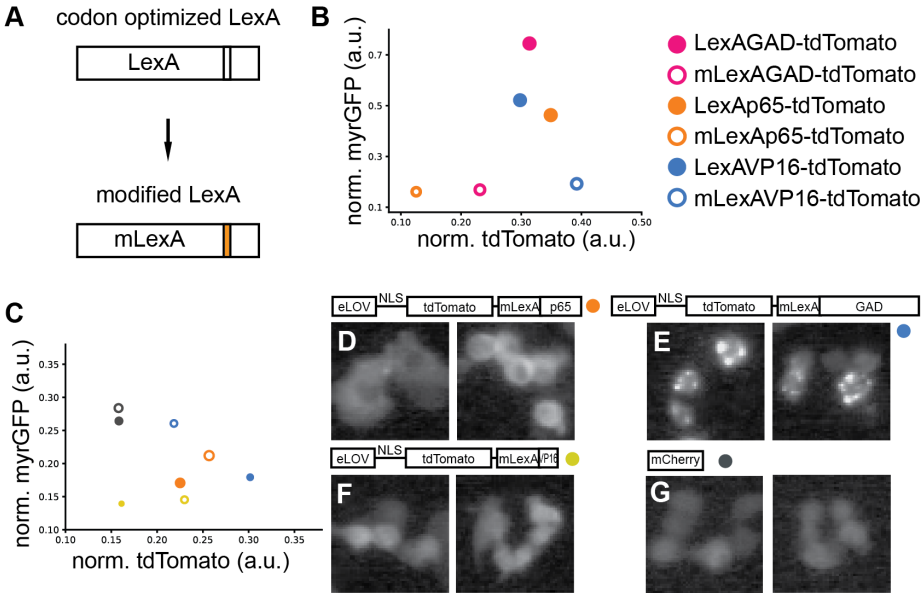

Figure 1: Testing components for a light-gated expression system based on eLOV. A. Schematic showing modified LexA. **B.** Expression of a LexAop reporter myr:GFP (measured by the ratio of myr:GFP signal/background signal) in relation to expression of LexA-transactivator chimera construct (ratio of tdTomato signal/background signal) for the different LexA- and mLexA-transactivator chimeras shows that mutagenizing NLS-like sequence reduces transcriptional activity of mLexA-transactivator chimeras (empty) compared to LexA-transactivator chimeras (filled). The size of the circle is proportional to the standard deviation of the cell population. **C.** Expression of reporter myr:GFP in relation to expression of mLexA-transactivator chimeras combined with eLOV, as in B. Placement of eLOV-nls N-terminal followed by the fluorescent protein tdTomato and the mLexA-transactivator chimera yielded the best signal for cells exposed to pulses of blue light, while maintaining a low reporter signal in cells kept in the dark. Constructs eLOV-nls-tdTomato-mLexAp65 and eLOV-nls-tdTomato-mLexAVP16 yielded the strongest increase in reporter expression upon exposure to blue light. **D - G.** S2R+ cells expressing eLOV-nls-tdTomato-mLexAp65 (D), eLOV-nls-tdTomato-mLexAGAD (E), eLOV-nls-tdTomato-mLexAVP16 (F) and mCherry (G) showing subcellular distribution of each of these constructs. The eLOV-nls-tdTomato-mLexAGAD combination forms clusters in the cytoplasm, whereas both eLOV-nls-tdTomato-mLexAp65 and eLOV-nls-tdTomato-mLexAVP16 are evenly distributed in the cytoplasm, and sometimes nucleoplasm, like mCherry.

To build a transcription factor gated by light, we selected the binary expression system LexA/LexAop [15, 61, 93], that is complementary to widespread the UAS-GAL4 system and has been successfully incorporated in diverse model organisms [15, 94, 95]. LexA is a repressor of transcription endogenous to *Escherichia coli* [65], where it regulates the SOS response [68]. Addition of an activation domain to the C-terminal of LexA renders such LexA-transactivator chimeras capable of activating transcription of transgenes sitting downstream of the LexA operator (LexAop) [15, 67]. In *Drosophila*, the most common LexA-transactivator chimeras contain the activation domains GAL4 activation domain (GAD, LexA:GAD), human p65 (LexA:p65) or VP16 (LexA:VP16) [15, 61, 67, 94]. Despite its bacterial origin, the LexA carries an NLS-like sequence that allows it to shuttle to the nucleus when expressed in eukaryotic cells [66, 67, 92]. To make translocation of LexA to the nucleus solely dependent on eLOVnls, we mutagenized the NLS-like sequence in the LexA codon optimized for *Drosophila melanogaster* [67, 92], and created a modified LexA (mLexA) (Figure 1A, see Materials and Methods). We examined the propensity to translocate to the nucleus of mLexA-transactivator chimeras by transfecting such constructs into the S2R+ *Drosophila* cell line [96], together with the metallotheionein-GAL4 (Met-GAL4) that drives ubiquitous expression upon addition of $CuSO_4$ [97], and the reporter myr:GFP under control of LexAop sequences [92]. All three chimeras of unmodified LexA-transactivator drove expression of the myr:GFP (Figure 1B), confirming their ability to shuttle to the nucleus [66, 67, 92]. In contrast, mLexA-transactivator chimeras led to reduced expression of the reporter transgene (Figure 1B), confirming that the NLS-like sequence in LexA is the main responsible for shuttling LexA to the nucleus.

We combined eLOVnls with the three mLexA-transactivator chimeras, and a fluorescent protein [98], placed each combination under control of the upstream activating sequence (UAS) and tested their performance in S2R+ cells co-transfected with Met-GAL4 and LexAop-myrGFP. Several of the mLexA constructs carrying eLOVnls C-terminally led to expression of myr:GFP in the dark (Figure S1A,B), indicating that NLS is frequently uncaged with eLOVnls at the C-terminal end, even in the absence of light delivery. On the other hand, many of the mLexA constructs with eLOVnls N-terminal were unable to drive expression of myr:GFP upon presentation of blue light (Figure S1A,B). The combinations made with LexAGAD chimera formed clusters in the cytoplasm (Figure 1E, S1C,D), while most other combinations were homogenously distributed in the cytoplasm and sometimes nucleoplasm (Figure 1D,F,G, S1E-I). Of note, cells with high levels of expression of many of the mLexA constructs tested, presented expression of myr:GFP irrespective of the light regime delivered (data not shown), indicating that eLOV is unstable if expressed at high levels, as previously observed [83, 90]. Cells expressing eLOVnls-tdTomato-mLexAp65 and eLOVnls-tdTomato-mLexAVP16 at moderate levels, presented no to very little LexAop-myr:GFP expression in the dark, and led to increase in expression of myr:GFP upon exposure to blue light (Figure 1C). These two constructs thus gathered the characteristics necessary for a light-gated expression system and were used to create transgenic flies. In addition, the eLOVnls-tdTomato-mLexAGAD was also injected since the mLexA-transactivator chimera LexAGAD is suppressible by Gal80, and could potentially provide another level of regulation of a light-gated expression system.

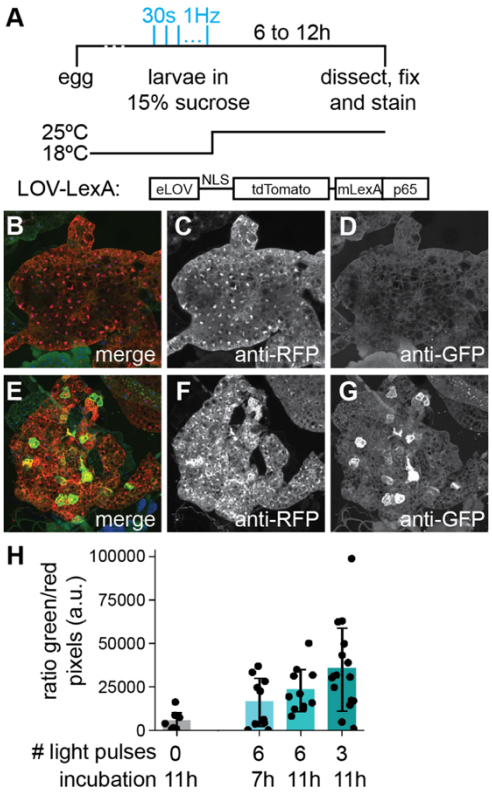

Figure 2. LOV-LexA is gated by light in vivo. A. Schematics showing the timeline of the experiment, light regime as well as the construct selected for LOV-LexA. **B-G.** Fat bodies of second to third instar larvae with LOV-LexA expression controlled by Cg-GAL4 for larvae kept in the dark (B-D) and exposed to three 30s pulses of blue LED light at 1 Hz (E-G). Exposure to blue light appears to alter LOV-LexA cellular distribution (C, F) and leads to expression of LexAop-CsChrimson:Venus in fat body cells as detected with anti-GFP antibody (D, G). **G.** Exposure to blue light leads to an increase in the amount of green signal, derived from CsChrimson:Venus compared to the LOV-LexA signal, measured by the ratio of anti-GFP signal/anti-RFP signal.

Characterization of eLOVnls-tag-mLexA chimera constructs in vivo

Drosophila larvae have transparent cuticle that allows for internal tissues to be exposed to unabated light. The bilateral, multilobed fat body running along the larva, is visible underneath the body wall musculature, and is targeted by the collagenase enhancer (Cg-)GAL4 [99]. Distribution of eLOVnls-tdTomato-mLexAGAD, eLOVnls-tdTomato-mLexAp65 or eLOVnls-tdTomato-mLexAVP16 in larval fat body followed the trend observed in S2R+ cells, with eLOVnls-tdTomato-mLexAGAD forming clusters (Figure S2A,C,D) and eLOVnls-tdTomato-mLexAp65 or eLOVnls-tdTomato-mLexAVP16 distributed evenly in the cytoplasm, and occasionally in the nucleoplasm (Figures 2B,C, S2B,F,G). To test the ability to induce expression of a reporter under control of LexAop sequences, LexAop-CsChrimson:Venus (hereafter referred to as Venus), second and third instar larvae reared at 18ºC, were placed in 96 well plates in a 15% sucrose solution, to repress their tendency to wonder, and exposed to several pulses of low intensity blue light (Figure 2A). Larvae were then incubated at 25ºC for 6 to 12 hours, fixed and stained. Despite considerable expression of eLOVnls-tdTomato-mLexAGAD and eLOVnls-tdTomato-mLexAVP16 in fat body cells, exposure to blue light failed to elicit expression of the reporter (Figure S2C-P). In contrast, exposure of larvae expressing eLOVnls-tdTomato-mLexAp65 to as little as 3 pulses of blue light led to increase in the reporter gene under control of LexAop sequences (Figure 2B-H). Surprisingly, a lower number of pulses of blue light combined with longer incubation at 25ºC resulted in maximum increase in reporter expression (Figure 2H), suggesting that despite low intensity, exposure to too much blue light leads to less efficiency of light-gated expression. Given that expression of eLOVnls-tdTomato-mLexAp65 in S2R+ and fat body cells kept in the dark presented no or very low expression of the reporter gene and that exposure

to light led to increase in reporter expression, the construct eLOVnls-tdTomato-mLexAp65 was selected for further studies and named LOV-LexA.

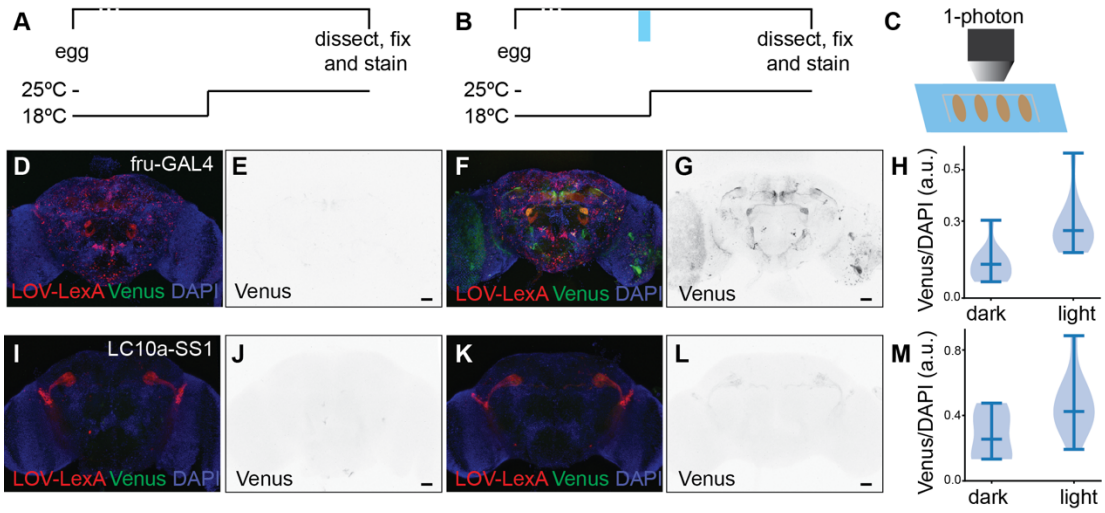

Figure 3: LOV-LexA gates expression with light in neurons. A, B. Timeline showing temperature and time of light delivery. **C.** Schematic showing how light was delivered to pupae. **D - G.** Adult brains showing native expression of LOV-LexA (red in D and F) and LexAop-CsChrimson:Venus (Venus, green in D and F, and dedicated image in E and G) from *fru-GAL4>LOV-LexA*, *LexAop-CsChrimson:Venus* pupae kept in the dark (D, E) or exposed to light at 3-4 days APF (F, G), as shown in B. **H.** Ratio of Venus signal intensity over DAPI signal intensity for *fru+* neuronal cell bodies located in the anterior brain. Flies exposed to pulses of blue light express the LexAop reporter Venus at higher levels, demonstrating that exposure to light leads to higher LOV-LexA transcriptional activity. **I - M.** Adult brains showing native expression of LOV-LexA (red in I and K) and LexAop-CsChrimson:Venus (Venus, green in I and K, and dedicated image in J and L) from *LC10a-SS1>LOV-LexA, LexAop-CsChrimson:Venus* pupae kept in the dark (I, J) or exposed to light at 3-4 days APF (K, L), as shown in B. **M.** Ratio of Venus signal intensity over DAPI signal intensity for LC10a neuronal cell bodies. Flies exposed to pulses of blue light express the LexAop reporter Venus at higher levels, demonstrating that exposure to light leads to higher LOV-LexA transcriptional activity.

LOV-LexA behavior in diverse neuronal types

Similar to fat body, we assessed LOV-LexA behavior in neurons with the transgene Venus under control of LexAop sequences (LexAop-CsChrimonson:Venus) [100] as a reporter of LOV-LexA transcriptional activity. Presence of CsChrimson:Venus is readily detected in its native expression in neurons with fixation alone (Figure S3A-J), thereby eliminating the need for the extra amplification step of antibody immunostaining [101]. We tested LOV-LexA in the lobula columnar 10 (LC10)-group neurons, LC10a, b, c, and d, that arborize in the lobula and project to anterior optic tubercle, a small region in the dorsal fly brain [26, 102-104]. LC10a neurons, but not LC10b, c, or d, mediate tracking of visual objects [20, 105]. Expression of LOV-LexA in LC10-group neurons with *LC10s-SS2* and *LC10a-SS1* drivers [20] led to moderate expression of Venus in the dark if flies were raised at 25ºC (Figure S3A-E), but not if flies were raised at 18ºC in the dark (Figure S3F-J). This indicates that if LOV-LexA is present at high levels, the dark state is leaky and allows for translocation of LOV-LexA to the nucleus in the absence of light, as observed in S2R+ cells (Figure S1) and in other systems based on eLOV [83, 90]. The stability of LOV-LexA in the dark was further tested with the panneuronal driver *GMR57C10-GAL4* [11]. In most neuron types, rearing flies at 18ºC prevented

accumulation of the Venus reporter in flies expressing LOV-LexA panneuronally (Figure S3K-M). A handful of neuron types, including neurons in the optic lobe, mushroom body, antennal lobe and suboesophageal region, were an exception to this rule and presented high levels of Venus expression. Differences in expression strength across neuron types represented in the *GMR57C10-GAL4* expression pattern may account for part of the observed variability in Venus expression in the dark. In contrast, αβ α'β' Kenyon cells in the mushroom body, the learning and memory center in the fly brain [106], appear to be weakly represented in *GMR57C10-GAL4* expression pattern, yet boast high levels of Venus in flies raised at 18ºC in the absence of light delivery (Figure S3K-M). Differential expression pattern of proteins involved in nucleocytoplasmic transport in different neuron types could potentially underlie these discrepancies. The α importin *a Karyopherin 4* (*aKap4*, CG10478) is highly expressed in Kenyon cells and other neuron types (Figure S3N) [107, 108]. Alpha importins function as adaptors that bind NLS peptides, bring proteins carrying an NLS close to the β importins that mediate their transport into the nucleus. The higher expression levels of *aKap4*, as well as that of other α and ß importins, in αβ Kenyon cells could potentially explain the leakiness of LOV-LexA dark state in these cells. To test this, we co-expressed *karyopherin-a1* (*Kap-a1*, CG8548) [108, 109] with LOV-LexA in LC10a-SS1 neurons in flies reared at 18ºC in the dark. In this case, LC10a-SS1 neurons exhibited expression of Venus reporter gene (data not shown), suggesting that increase in nucleocytoplasmic transport, as the one elicited by over-expression of *Kap-a1*, may facilitate translocation of LOV-LexA to the nucleus, in the absence of light delivery.

We tested several GAL4 and split-GAL4 drivers in flies raised at 18ºC and compared native expression of LOV-LexA and the reporter Venus. Like in other cell types, above certain levels of expression of LOV-LexA, the amount of Venus detected in neurons correlated with that of LOV-LexA (Figure S3O,P). Together these observations suggest that the LOV-LexA tool has a stable dark state in drivers of weak to moderate expression strength, which constitute the majority of GAL4 and split-GAL4 lines available for genetic access to single neuron types [11, 14, 21, 24-42].

LOV-LexA mediates light-gated expression in neurons

The pupal case and the adult cuticle are tanned and block light, leading to decreased exposure of internal tissues to light. To uncage the NLS in LOV-LexA expressed in pupal and adult brain, we used a 1-photon laser with 458 nm wavelength in a confocal microscope (see Materials and Methods). The driver *fru-GAL4*, a *GAL4* knock-in in the locus of the gene *fruitless* (*fru*) [110, 111], targets approximately 100 neuron types, together called *fru* neurons, many of which were shown to regulate courtship behavior [among others, 20, 101, 112, 113-118]. Expression is initiated in pupal development with low expression strength at late pupal stages. Pupae reared at 18ºC and expressing LOV-LexA in *fru* neurons, were lined-up on a double-side sticky tape on a coverslip mounted on a slide and exposed to a series of four to six pre-programmed light pulses, after which they were placed at 25ºC for two to four days (Figure 3A-C). Expression of Venus was significantly increased in most *fru* neurons in pupae that were exposed to blue light (Figure 3D-H). Importantly, pupae kept in the dark displayed little or no expression of Venus (Figure 3D,E,G). Similar outcomes were observed for the *LC10a-SS1* driver. Like *fru-GAL4*, *LC10a-SS1* drives expression in pupal stages at low levels [20,

and data not shown]. Exposure of pupae to four pulses of 1-photon laser 458nm light spaced over 30 minutes, elicited expression of Venus in LC10a neurons (Figure 3I-M). Pupae mounted on the same slide, but kept in the dark, did not present expression of Venus. Increase in expression of the reporter Venus in fru+ and LC10-group neurons exposed to light, and its absence in the same neurons kept in the dark, demonstrates that LOV-LexA gates expression with blue light in neurons in the pupal fly brain.

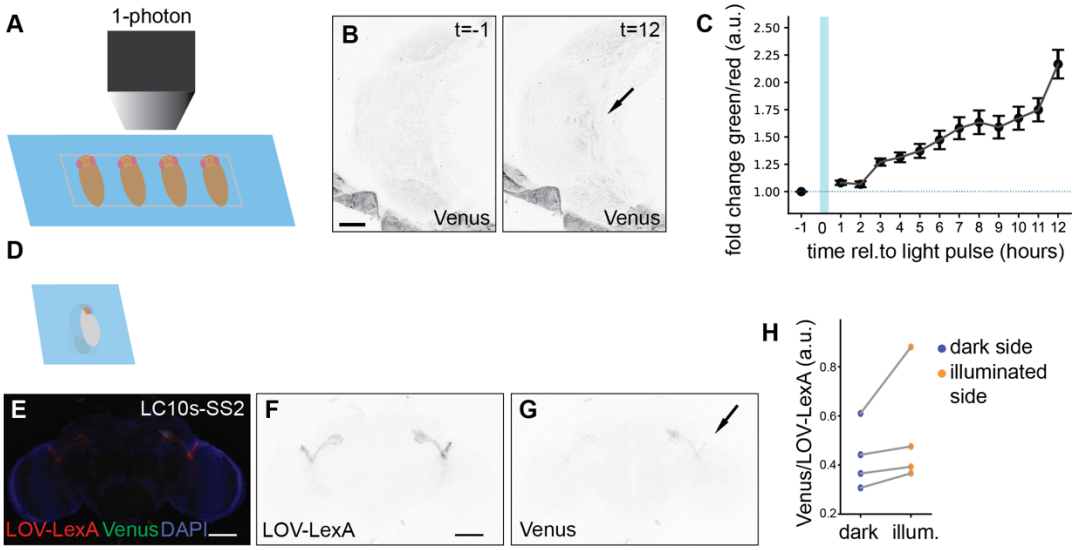

Figure 4: LOV-LexA enables spatial and temporal control of transgene expression with light.
A. Schematic showing the set-up to expose pupal heads lined up on a slide, to blue light. **B.** Live image of a 4d APF pupal head after removal of the pupal case, with expression of Venus in fru+ neurons before delivery of blue light (left panel) and 12 hours after delivery of blue light (right panel). **C.** Change in the ratio of native Venus signal over LOV-LexA tdTomato native signal, before and after light delivery. **D.** Schematic showing preparation to deliver spatially restricted light to immobilized adult flies. **E-G.** Representative image of an adult brain expressing LOV-LexA (red in E, dedicated image F) in LC10s-SS2 neurons, and LexAop-CsChrimson:Venus (green in E, dedicated image G) unilaterally, after exposure to spatially restricted blue light to target LC10-group neurons unilaterally. **H.** Graph showing difference in ratio of native Venus signal/native tdTomato (LOV-LexA) signal between the side of the head that was illuminated compared to the side that was kept in the dark.

Precise control of the time of initiation of transgene expression has numerous advantages, including allowing for embryonic and pupal development to occur undisturbed in the absence of ectopic expression and for regulation of the level of transgene expressed. We measured the time it takes for LOV-LexA to drive transcription of LexAop controlled Venus after exposure to blue light. The head in pupae expressing LOV-LexA with *fru-GAL4* was uncovered by removing the encapsulating pupal case and exposed to pulses of blue light as previously (Figure 3B, 4A). The pupal brain was then imaged every hour for 12 hours to determine the timing at which Venus starts to be expressed. Venus expression doubled 12 hours after blue light pulse delivery (Figure 4B,C). Detection of expression with native protein fluorescence in adult brains was reliably observed 24 hours after exposure to blue light during late pupal stages (Figure 3D-H), indicating that LOV-LexA light-gated expression takes 12 to 24 hours to accumulate enough LexAop Venus reporter to be visualized with native levels.

Drivers that initiate expression at adult stages, such as LC10s-SS2, have to be exposed to light at adult stages. Adult flies expressing LOV-LexA in LC10-group neurons were immobilized with low-melting wax and covered with plasticine, leaving uncovered only the area of cuticle above the cells of interest (Figure 4D), as a manually inserted additional pinhole. Somata for the LC10-group neurons are located in the dorso-posterior side of the head, in an area bordering the rim of the retina. Immobilized flies with the cuticle covering somata of LC10-group neurons on one side of the adult head exposed, were delivered six pulses of 458nm 1-photon laser light over the course of one hour. Detection of native fluorescence revealed accumulation of Venus in LC10-group neurons exclusively on the side exposed to light (Figure 4E-G). Importantly, most flies prepared in this fashion showed unilateral expression in LC10-group neurons (Figure 4H), indicating that LOV-LexA allows for consistent genetic access to the same subsets of cells within an expression pattern.

Discussion:

We developed LOV-LexA, a light-gated expression system based on the photosensitive eLOV domain [86], and the transcription factor chimera mLexAp65 [92, 94]. In the absence of light, LOV-LexA proteins reside in the cytoplasm of larval and adult cell types. Delivery of blue light causes the LOV Jα helix to uncage a NLS, which then mediates translocation of the transcription factor to the nucleus. Once in the nucleus, LOV-LexA drives expression of transgenes under control of LexAop sequences. The use of light as a trigger enables control of expression with high spatial and temporal resolution in live adult animals, making LOV-LexA an important addition to the *Drosophila* genetic toolbox that will expand the use of existent broadly expressed drivers as well as allow for assessing subsets of cells within one single cell type with unrivaled consistency.

Several forms of LexA-transactivator chimeras are used in different animal models [15, 94, 95]. Surprisingly, the ability to remain outside the nucleus in the dark and to elicit reporter expression upon light exposure varied widely among different combinations of mLexA-transactivator chimeras, eLOV-nls and tag. For instance, replacing tdTomato with the FLAG tag in the LOV-LexA construct to make eLOV-nls-FLAG-mLexAp65, leads to high levels of leakiness in the dark in S2R+ cells, suggesting that intra-protein interactions among the different components of LOV-LexA play an important role in stability of the Jα helix in the dark [83, 86].

At high levels of expression, LOV-LexA proteins translocate to the nucleus and drive expression of the LexAop reporter transgene, imposing limits on the temperature used to raise fruit flies and the available driver lines. Further improvements of the eLOV domain have to be implemented to circumvent this limitation [90]. On the other hand, some neuron types present LexAop reporter expression even if LOV-LexA is expressed at low levels. The uneven expression of α importin *aKap4* across neuron types in the fly brain, similar to what is observed in the mouse brain for all importins [119], suggests that different neuron types might express protein machinery supporting nucleocytoplasmic transport to different extents. We predict that this variability is likely to influence how LOV-LexA functions across neuron types, making neurons with high nucleocytoplasmic transport capabilities unsuitable for light-gated expression with LOV-LexA.

Other light-gated expression systems have been developed in *Drosophila*, including the cryptochrome split-LexA and Photo-Gal4 [59, 60]. We expressed the cryptochrome split-LexA with the same driver used to test LOV-LexA, LC10s-SS2 [20], and found that cryptochrome split-LexA system is leaky in flies raised at 18ºC and kept in the dark (data not shown). The spatial resolution provided by Photo-GAL4 remains unmatched by LOV-LexA *in vivo*, due to the scattering that occurs once light traverses the cuticle in pupal and adult flies. Given that Photo-GAL4 relies on PhyB and requires addition of the chromophore PCB, normally absent in animal cells, it is currently limited to *ex vivo* studies [59]. The chromophore providing LOV with light sensitivity is flavin mononucleotide that exists in animal cells, making the LOV-LexA system solely dependent on delivery of light.

There are thousands of enhancer-LexA or -GAL4 drivers targeting several cell types simultaneously [11, 14, 27, 120, 121]. The LOV-LexA can be placed downstream of broadly expressed enhancers,

in order to elicit transgene expression in the neuron type of interest with delivery of light specifically to its somata. Replacing the exogenous transcription factor, GAL4 or LexA, in existent GMR and VT enhancers with LOV-LexA will thus expand the number of single neuron types genetically accessible and contribute to delineate neural circuits and decipher their functions. LOV-LexA placed downstream of an enhancer can be combined with GAL4 and QF binary expression systems, to genetically target two or more single neuron types independently in the same animal, enabling simultaneous monitoring of neuronal activity or determining dependency relationships among different neuron types with neuronal epistasis.

Many neuron types are composed of dozens of cells that are topographically organized to represent visual field [26, 102, 122]. Topographic organization of neuropiles processing sensory information is also observed in other animals, like the mouse superior colliculus, visual cortex, and for other sensory modalities, like the barrel cortex [123-125], among others. LOV-LexA is an ideal tool to test the role of topography, by providing genetic access consistently to the same subsets of somata within a single neuron type, with minimal stochasticity. Since LOV-LexA accumulates in the cell bodies and travels little to dendrites and axons, targeting light to the topographically organized neuronal processes yields little increase in expression. We demonstrate consistent targeting of LC10-group neurons unilaterally with LOV-LexA by targeting their somata. Applying this strategy to all visual projection neurons will elucidate how each contributes to guiding visual behavior.

Roughly 12 to 24 hours separate delivery of blue light for eliciting expression with LOV-LexA and accumulation of transgene expression in neurons, giving the fly time to recover from potential adverse effects of delivery of blue light, that include temporary blindness [126]. This time separation also allows for more light and genetic manipulations to be performed on the same animal, without the need to perform all light-dependent manipulations on the tethered fly [127]. Targeting a specific neuron type with LOV-LexA together with providing shaped light to a tethered fly, targeting another neuron type with genetic access with an independent binary system [127], brings the possibility of testing subsets of neuronal cells of two multicellular neuron types accessed independently and simultaneously in the same animal.

Compared to *Drosophila melanogaster*, many model organisms in which it is possible to apply genetics, have smaller repertoires of enhancer driver lines that give access to different tissues and cell types. Implementing LOV-LexA in such model organisms will greatly amplify the number of specific cell types that can be genetically manipulated, expanding the landscape of possible experiments in emerging model organisms and the knowledge we can acquire from them.

Materials and Methods:

Table 1. Genetic constructs used in this study.

Name	Features	Vector	Promoter	Details
c204	tdTomato-mLexA:GAD	pJFRC7	UAS	modified LexA:GAD codon optimized for *Drosophila*
c205	tdTomato-LexA:GAD	pJFRC7	UAS	LexA:GAD codon optimized for *Drosophila*
c214	tdTomato-mLexA:p65	pJFRC7	UAS	Modified LexA:p65 codon optimized for *Drosophila*
c215	tdTomato-LexA:p65	pJFRC7	UAS	LexA:p65 codon optimized for *Drosophila*
c224	tdTomato-mLexA:VP16	pJFRC7	UAS	Modified LexA:VP16 codon optimized for *Drosophila*
c225	tdTomato-LexA:VP16	pJFRC7	UAS	LexA:VP16 codon optimized for *Drosophila*
c11	eLOV-nls-tdTomato-mLexA:GAD	pJFRC7	UAS	LexA:GAD codon optimized for *Drosophila*, with NLS-like modified
c12	eLOV-nls-tdTomato-mLexA:p65	pJFRC7	UAS	LexA:p65 codon optimized for *Drosophila*, with NLS-like modified
c13	eLOV-nls-tdTomato-mLexA:VP16	pJFRC7	UAS	LexA:VP16 codon optimized for *Drosophila*, with NLS-like modified
c17	mLexA:GAD-tdTomato-eLOV-nls	pJFRC7	UAS	LexA:GAD codon optimized for *Drosophila*, with NLS-like modified
c18	mLexA:p65-tdTomato-eLOV-nls	pJFRC7	UAS	LexA:p65 codon optimized for *Drosophila*, with NLS-like modified
c19	mLexA:VP16-tdTomato-eLOV-nls	pJFRC7	UAS	LexA:VP16 codon optimized for *Drosophila*, with NLS-like modified
c111	ceLOV-nls-tdTomato-mLexA:GAD	pJFRC7	UAS	LexA:GAD codon optimized for *Drosophila*, with NLS-like modified eLOV evolved LOV codon optimized for *Drosophila*
c121	ceLOV-nls-tdTomato-mLexA:p65	pJFRC7	UAS	LexA:p65 codon optimized for *Drosophila*, with NLS-like modified eLOV evolved LOV codon optimized for *Drosophila*
c131	ceLOV-nls-tdTomato-mLexA:VP16	pJFRC7	UAS	LexA:VP16 codon optimized for *Drosophila*, with NLS-like modified eLOV evolved LOV codon optimized for *Drosophila*
c26	mLexA:GAD-GFP-eLOV-nls	pJFRC7	UAS	LexA:GAD codon optimized for *Drosophila*, with NLS-like modified

Name	Features	Vector	Promoter	Details
c27	mLexA:p65-GFP-eLOV-nls	pJFRC7	UAS	LexA:p65 codon optimized for *Drosophila*, with NLS-like modified
c28	mLexA:VP16-GFP-eLOV-nls	pJFRC7	UAS	LexA:VP16 codon optimized for *Drosophila*, with NLS-like modified
c29	mLexA:GAD-GFP-ceLOV-nls	pJFRC7	UAS	LexA:GAD codon optimized for *Drosophila*, with NLS-like modified eLOV evolved LOV codon optimized for *Drosophila*
c30	mLexA:p65-GFP-ceLOV-nls	pJFRC7	UAS	LexA:p65 codon optimized for *Drosophila*, with NLS-like modified eLOV evolved LOV codon optimized for *Drosophila*
c31	mLexA:VP16-GFP-ceLOV-nls	pJFRC7	UAS	LexA:VP16 codon optimized for *Drosophila*, with NLS-like modified eLOV evolved LOV codon optimized for *Drosophila*
myr:Tom	LexAop-myr::tdTomato	pJFRC19	LexAop	LexAop driving tdTomato expression; reporter for activity of LexAxx-eLOV-tag with GFP or FLAG
mCherry	mCherry	pJFRC7	UAS	UAS driving mCherry expression; reporter for transfection efficiency and negative control for LexAxx-eLOV-tag constructs
myrGFP	LexAop-myr::GFP	pJFRC19	LexAop	Pfeiffer, et al, 2008 and 2010 Addgene # 26224
CD8:GFP	CD8:GFP	pJFRC7	UAS	Pfeiffer, et al, 2008 and 2010 Addgene # 26220

Plasmids and cloning:

The LexA chimeras LexA:GAD, LexA:p65 and LexA:VP16 from the plasmids pBPLexA::GADUw, pBPLexA::p65Uw and pBPLexA::VP16Uw (Addgene # 26230, 26231, 26232, Gerald Rubin lab) were mutagenized to change the NLS-like sequence from: (2433) GTT ACT GTG AAA CGT CTC AAG AAG CAA GGC AAT (VTVKRLKKQGN), to: (2433) GTT ACT GTG AAA GGG CTC GAG AAG CAA GGC AAT (VTVKGLEKQGN) [67], using a kit (Q5 site directed mutagenesis kit from New England Biolabs). The resulting modified LexA (mLexA) chimeras were combined through DNA assembly [128] with the following components: eLOV (Addgene # 92213, Alice Ting lab) [86], SV40 nuclear localizing signal [92] and tdTomato [98] or GFP (from pJFRC7-20XUAS-IVS-mCD8::GFP , Addgene # 26220, Gerald Rubin lab) [10] or FLAG (amino acid sequence: DYKDDDDK) with a kit (Gibson assembly kit from New England Biolabs). The different combinations were cloned into pJFRC7-20XUAS-IVS-mCD8::GFP (Addgene # 26220) cut with XhoI and XbaI, to replace mCD8::GFP, and produce pJFRC7-20XUAS-LexAxx-eLOV-tag construct combinations.

S2R+ cell culture, transfection, stimulation, fixation and immunostaining:

The *Drosophila* cell line S2R+ [96] was obtained from the *Drosophila* Genomics Resource Center, supported by NIH grant 2P40OD010949. S2R+ cells cultured at 25ºC in Schneider's Medium (Gibco) containing 10% fetal bovine serum (Gibco) and 1% penicillin-streptomycin (Gibco). To test the various LexAxx-eLOV-tag constructs, listed in Table 1, for cell survival and ability to drive expression gated by light, S2R+ cells were transfected with pMET-GAL4 as the driver, the UAS-LexAxx-eLOV-tag test construct, and pJFRC19-13XLexAop2-IVS-myr::GFP (Addgene #26224) or 13XLexAop-IVS-myr::tdTomato (this study) as the LexAop-led reporters of LexAxx-eLOV-tag transcriptional activity. We used co-transfection of pMET-GAL4 [97], pJFRC7-20XUAS-IVS-mCD8::GFP [10], pJFRC7-20XUAS-IVS-mCherry [this study] as controls to characterize transfection efficiency of three constructs. Three DNA plasmids, 200 to 250ng/ul, were combined with FuGene (HD Transfection from Promega) in Schneider's media with a proportion of 600 to 750 ng DNA for 4ul FuGene. The DNA plasmid/FuGene mix was allowed to stand for 30 minutes to one hour at room temperature, after which it was added to roughly 1 million cells pre-plated in a 24-well plate. The metallothionein promoter in the pMET-GAL4 driver [97] is activated by addition of copper sulfate ($CuSO_4$), to a final concentration of 0.75 mM. Presentation of light was initiated 1 to 3 hours after addition of copper sulfate. Light was delivered in pulses of 30s of blue LED (from the LED light source of the inverted laboratory microscope LEICA DM IL LED) at 1 Hz. Cells were fixed with 4% paraformaldehyde overnight at 4ºC, between 8 to 10 hours after addition of copper sulfate, and processed for immunostaining with standard protocols [for eg., 97], with antibodies anti-GFP chicken antibody dillution 1:2000 (Rockland, Catalogue # 600-901-215S; RRID: AB_1537403), anti-RFP rabbit antibody dilution 1:2000 (Rockland, Catalogue # 600-401-379, RRID: AB_11182807), anti-FLAG rat antibody dilution 1:300 (Novus Biologicals, Catalogue # NBP1-06712, RRID: AB_1625981). Secondary antibodies were goat anti-chicken Alexa Fluor 488 (1:1000), goat anti-rabbit Alexa Fluor 568 (1:1000) and goat anti-rat Alexa Fluor 568 (1:1000). Five images per well were obtained from immuno-stained cells with an inverted fluorescence microscope (Leica DM IL LED), with a 5x objective. The open-source software CellProfiler (version 4.1.3) [129] was used to segment individual cells based on the LexAxx-eLOV-tag signal and measure the amount of LexAop-reporter in each segmented cell, produced by transcription of LexAop-led reporters of LexAxx-eLOV-tag activity. Scripts written in Python (version 3.8, http://www.python.org) were then used to plot the data provided by CellProfiler.

***Drosophila* culture and genetics:**

Stocks obtained from the Bloomington Drosophila Stock Center (NIH P40OD018537) were used in this study. The strains of the fruit fly *Drosophila melanogaster* used in this study are listed in Table 2. Fruit flies were maintained on standard cornmeal-agar medium supplemented with baker's yeast and incubated at 18ºC or 25ºC with 60% humidity and 12h light/dark cycle. Males and females were tested indiscriminately throughout experiments. Larvae of the second and third instar were used for tests of LOV-LexA on fat body with *Cg-GAL4*; 3 to 4 days after puparium formation (APF) pupae

were used for LOV-LexA tests in muscle (*DMef2-GAL4*) and neurons (*fru-GAL4*); adults ranging from 1 to 6 days old were used for LOV-LexA tests in adult neurons.

Table 2. *Drosophila melanogaster* strains used in this study.

Drosophila melanogaster strains	Reference	Source
Cg-GAL4	Asha, et al, 2003	Bloomington Drosophila Stock Center
fru-GAL4	Stockinger, et al, 2005	-
GH86-GAL4	Bloomington Drosophila Stock Center	Bloomington Drosophila Stock Center
vGlut-GAL4	Bloomington Drosophila Stock Center	Bloomington Drosophila Stock Center
GMR57C10-GAL4	Jennet, et al, 2012	FlyLight, Janelia Research Campus
SS00324	Jennet, et al, 2012	FlyLight, Janelia Research Campus
LC10a-SS1	Ribeiro, et al, 2018	-
VT043656-GAL4	Tirian and Dickson, 2017	-
VT047880-GAL4	Tirian and Dickson, 2017	-
LC10s-SS2	Ribeiro, et al, 2018	-
UAS-LOV-LexA in attP1 su(Hw)	this study	-
UAS-eLOV-nls-tdTomato-mLexA:GAD in attP1 su(Hw)	this study	-
UAS-eLOV-nls-tdTomato-mLexA:VP16 in attP1 su(Hw)	this study	-
LexAop-CsChrimson:Venus in attP18	Klapoetke, et al 2014	Vivek Jayamaran, Janelia Research Campus
LexAop-myr:GFP	Pfeifer, et al, 2010	Gerald Rubin at Janelia Research Campus
$y^{1},w^{*};Mi[MIC]aKap4^{MI06313}$ $PVRAP^{MI06313}$	Venken, et al, 2011	Bloomington Drosophila Stock Center
w; P[UAS- Kap-a1.M]2*	Wharton, K. (2008.08.22) personal communication to FlyBase	Bloomington Drosophila Stock Center
w^{1118}*; M{[UAS- Kap-a1.HA]ZH-51C*	Wharton, K. (2008.08.22) personal communication to FlyBase	Bloomington Drosophila Stock Center

Stimulation of LOV-LexA *in vivo*:

To test UAS-LOV-LexA, UAS-eLOV-nls-tdTomato-mLexA:GAD and UAS-eLOV-nls-tdTomato-mLexA:VP16 constructs in fat body cells, second to third instar larvae from crosses with Cg-GAL4, were removed from the food, washed in water and placed in a well with 40 µl of 15% sucrose in water solution, one larva per well in a 96-well plate wrapped in aluminum foil to shield the larvae from ambient light. Pulses of light were delivered to individual wells, with the 96-well plate mounted on an inverted microscope with light from a blue LED (LEICA DM IL LED), for 30s at 1Hz. Larvae in half the plate was not exposed to light and served as controls. The fat bodies were dissected 6 to 12 hours after light delivery, fixed and immunostained with anti-GFP chicken antibody dilution 1:1000 (Rockland, Catalogue # 600-901-215S; RRID: AB_1537403) and anti-RFP rabbit antibody dilution 1:2000 (Rockland, Catalogue # 600-401-379, RRID: AB_11182807). Secondary antibodies were goat anti-chicken Alexa Fluor 488 (1:1000), goat anti-rabbit Alexa Fluor 568 (1:1000). Stained fat bodies were mounted with Vectashield Antifade Mounting Medium (Vector Laboratories) and imaged with a Leica TCS SP8 confocal microscope.

To recover pupae from crosses, water was added to the walls of the vial to dissolve the glue binding pupal cases to the vial wall. Pupae were dried on a kimwipe tissue and then glued on a double-side sticky tape spread on a cover slip, that was attached to a microscope slide with plasticine (Figure 4A). Adult flies were placed on a custom aluminum holder with a hole large enough to expose part of the head and the thorax of the adult fly, and shield the rest of the fly from light. Melted Eicosane 99% (Aldrich 219274-5G) was added to the thorax and part of the head to immobilize the adult fly and shield part of the head from light (Figure 4D). Such custom holders were mounted on a microscope slide with plasticine.

Slides bearing pupae or adult flies were then mounted on an upright confocal microscope (Leica TCS SP8) for pre-programmed serial light delivery with the 458nm laser at 10% power. Each light pulse was composed to 50 to 100 scans at 400Hz across a depth of 200 to 400 µm of the head for stimulation of neurons. Using the xyzt mode of Leica software together with position mapping, it was possible to deliver light serially to many pupae or adult flies at the same time. After light delivery, cover slips with pupae were vertically inserted into new food vials and incubated for 2 to 3 days for expression in neurons in the fly brain, before dissection. Adult flies were removed from holders after light delivery, by breaking the brittle Eicosane, placed in fresh food vials and incubated at 25ºC for 1 to 3 days before brain dissection.

Adult brains were dissected in cold PBS, fixed in 4% PFA, washed in PBS with 0.5% Triton X-100, incubated with DAPI at dilution 1:3000 in PBS with 0.5% Triton X-100, washed again and mounted with Vectashield Antifade Mounting Medium (Vector Laboratories) and imaged on the same day with a Leica TCS SP8 confocal microscope.

Images representing S2R+, fat body, live pupal heads and adult brains were processed with Fiji software [130].

Tool and data availability:

The DNA plasmid for LOV-LexA will be deposited in Addgene and is available upon request. The *Drosophila melanogaster* LOV-LexA fly lines will be deposited in Bloomington and in VDRC, and are also available upon request. Data sets are available upon request. Please contact Inês M.A. Ribeiro at ribeiroinesma@gmail.com.

Acknowledgements:

We are grateful to M.Sauter and C.Theile for technical assistance with fly husbandry, S.Prech and R.Kasper for assistance with sets ups to deliver light and the Imaging Facility, to R.Vieira for assistance with cloning, and to A.H.Ali and R.M.Vieira for critically reading the manuscript. The Bloomington Drosophila Stock Center, the *Drosophila* Genomics Resource Center, and FlyBase were instrumental for this research project and countless others, and the authors wish these institutions remain fully funded. This work was supported by the Max Planck Gesellschaft (to A.B., W.E. and R.K.) and Rosa-Laura und Harmut Wekerle Foundation (to I.M.A.R.).

Figure S1:

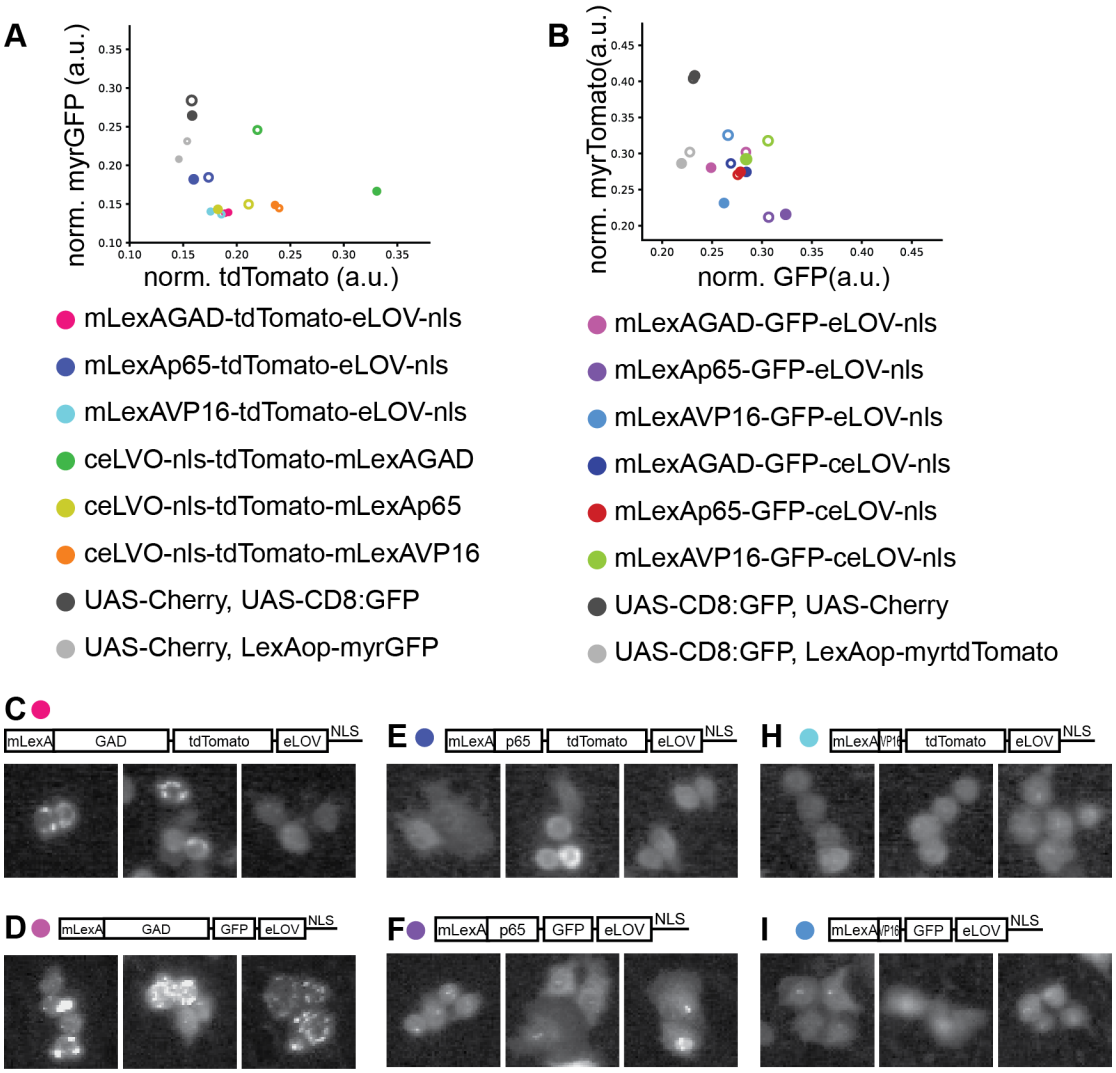

Figure S1: Design of a light-gated expression system based on LOV (suppl. to Figure 1). A. Expression of reporter myr:GFP (measured by the ratio of myr:GFP signal/background signal) in relation to expression of mLexA chimera-LOV construct (ratio of tdTomato signal/background signal) for the different combinations bearing tdTomato tested; filled circles for cells kept in the dark, empty circles for cells exposed to blue light. UAS-mCherry and UAS-CD8:GFP or UAS-mCherry and LexAop-mryGFP were used as controls. (ceLOV stands for eLOV codon optimized for *Drosophila*). **B.** Expression of the reporter myr:tdTomato (measured by the ratio of Tomato signal/background signal) in relation to expression of mLexA chimera-LOV combination (ratio of GFP signal/background signal) for the different combinations bearing GFP tested; filled circles for cells kept in the dark, empty circles for cells exposed to blue light. UAS- CD8:GFP and UAS-mCherry or UAS- CD8:GFP and LexAop-mryTomato were used as controls. None of the constructs tested in A or B elicit any light-dependent increase in LexAop-reporter transgene. **C-I.** S2R+ cells expressing mLexAGAD-tdTomato-eLOV-nls (C), mLexAGAD-GFP-eLOV-nls (D), mLexAp65-tdTomato-eLOV-nls (E), mLexAp65-GFP-eLOV-nls (F), mLexAVP16-tdTomato-eLOV-nls (H), mLexAVP16-GFP-eLOV-nls (I) showing subcellular distribution of each of these combinations. All combinations bearing LexAGAD form clusters in the cytoplasm, whereas combinations bearing LexAp65 or LexAVP16 are distributed evenly in the cytoplasm and nucleoplasm.

Figure S2:

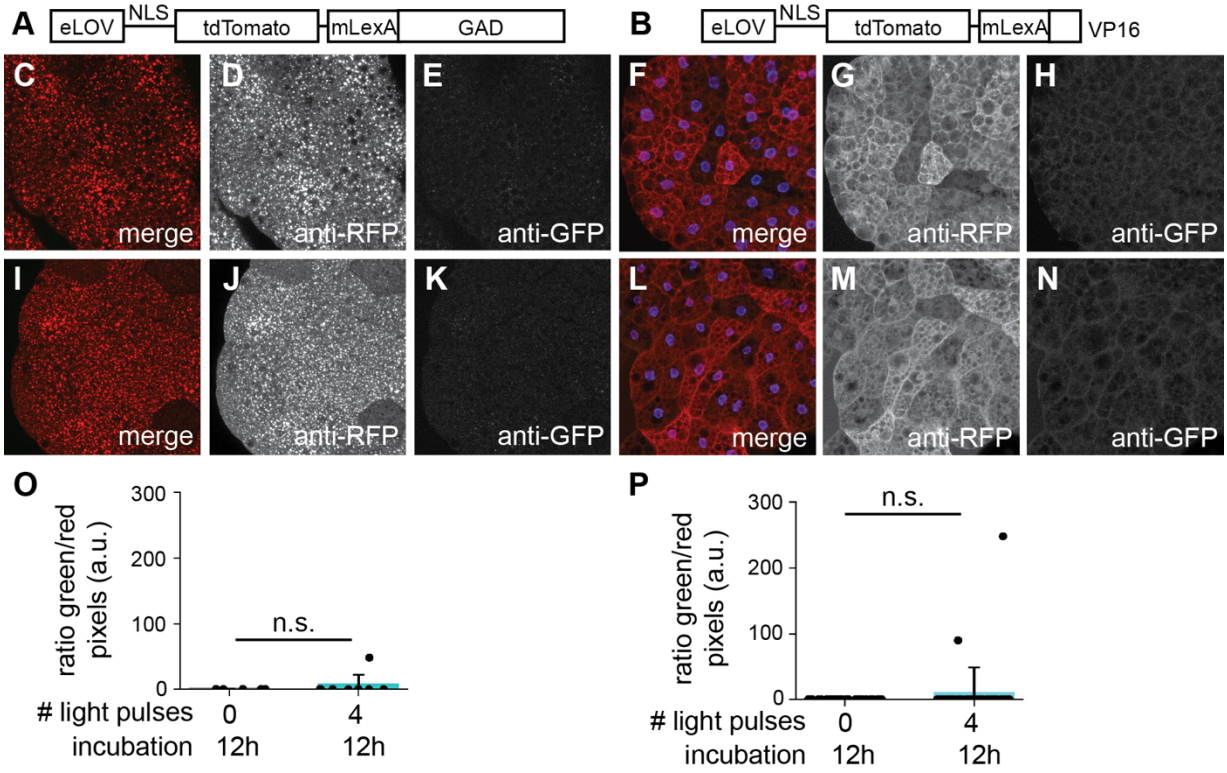

Figure S2: LexA chimeras LexAGAD and LexAVp16 combined with N-terminal eLOV are unable to elicit expression of LexAop transgene. A,B. Schematic of the constructs tested. **C-N.** Fat bodies of second to third instar larvae expressing eLOV-tdTomato-mLexAGAD (C-E,I-K) or eLOV-tdTomato-mLexAVP16 (F-H, L-N) with Cg-GAL4 for larvae kept in the dark (C-E, F-H) and exposed to three 30s pulses of blue LED light at 1 Hz (I-K, L-N). **O, P.** Quantification of the ratio of CsChrimson:Venus and tdTomato construct signal across different second to third instar larvae shows that eLOV-tdTomato-mLexAGAD and eLOV-tdTomato-mLexAVP16 do not gate expression of LexAop-reporter transgene with light.

Figure S3:

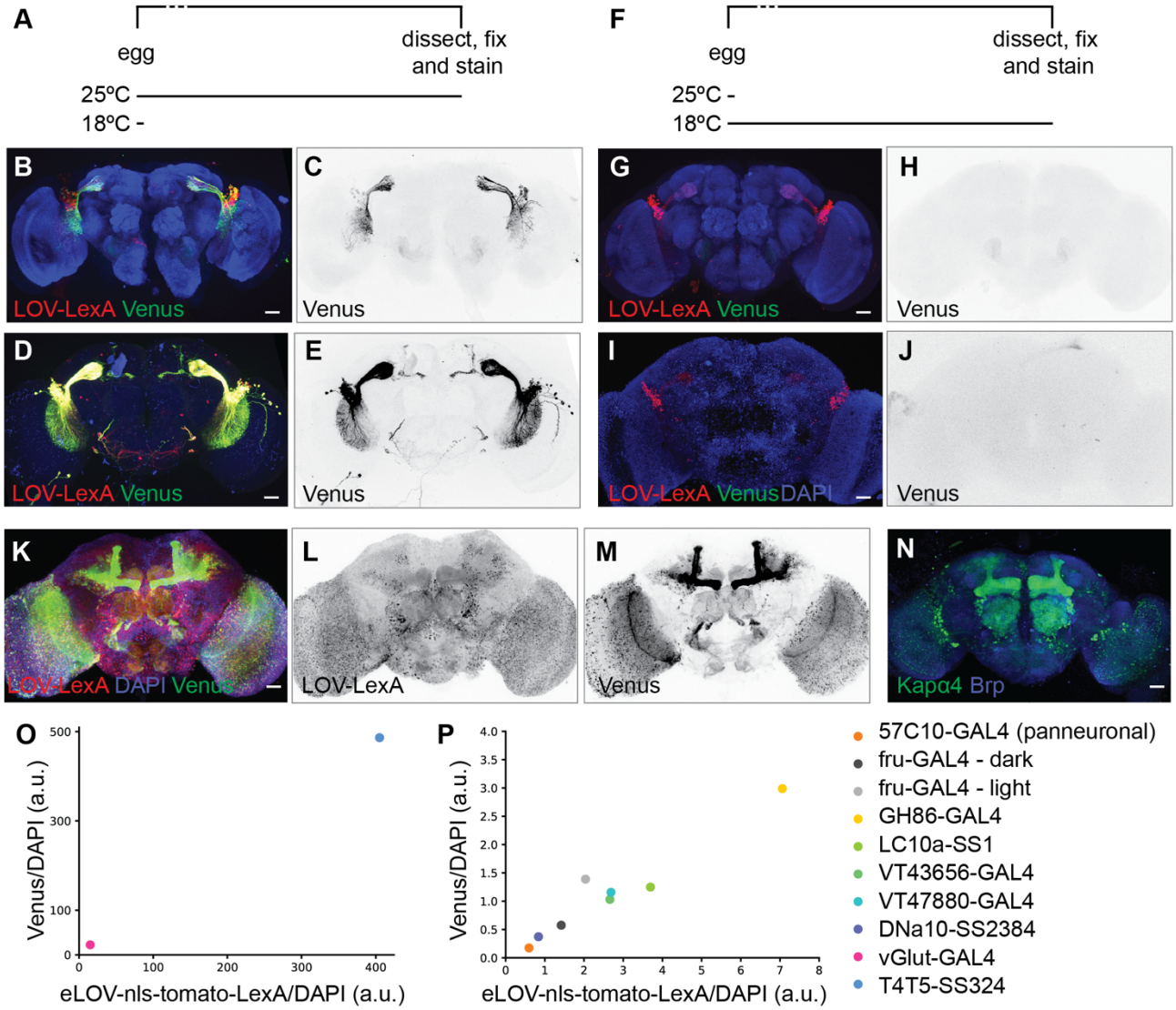

Figure S3: LOV-LexA tests in neurons. A. Schematic representing the timeline of fly rearing for the brains shown in B to E. **B-E.** LOV-LexA under control of *LC10s-SS2* (B) or *LC10a-SS1* (D) driver in flies reared at 25ºC shows expression of the LexAop-reporter transgene Venus (C, E). **F.** Schematic representing the timeline of fly rearing for the brains shown in G to J. **G-J.** LOV-LexA (G) under control of *LC10s-SS2* (G) or *LC10a-SS1* (I) driver in flies reared at 18ºC shows no expression of the LexAop-reporter transgene Venus (H, J). **K-M.** LOV-LexA (K, L) under control of a panneuronal driver GMR57C10-GAL4 showing LOV-LexA distribution predominantly in cell bodies (L) and uncorrelated expression of the LexAop-reporter Venus (M) in different neurons. **N.** Expression of the α importin *aKap4* with a MiMIC line inserted in the *aKap4* gene locus (*aKap4*^{MI06313}), demonstrating expression in specific neuron types, including Kenyon cells. **O.** Tests for the dark state of LOV-LexA for various drivers of different strength shows that above certain levels of expression, Venus expression correlates with LOV-LexA expression level in the dark state. If expressed at moderate to low levels, LOV-LexA maintains low transcriptional activity, that increases with light exposure, as is the case for *fru-GAL4*.

References:

1. Brand, A.H. and N. Perrimon, *Targeted gene expression as a means of altering cell fates and generating dominant phenotypes.* Development, 1993. **118**(2): p. 401-15.
2. Bellen, H.J., et al., *P-element-mediated enhancer detection: a versatile method to study development in Drosophila.* Genes Dev, 1989. **3**(9): p. 1288-300.
3. Grossniklaus, U., et al., *P-element-mediated enhancer detection applied to the study of oogenesis in Drosophila.* Development, 1989. **107**(2): p. 189-200.
4. Wilson, C., et al., *P-element-mediated enhancer detection: an efficient method for isolating and characterizing developmentally regulated genes in Drosophila.* Genes Dev, 1989. **3**(9): p. 1301-13.
5. Perrimon, N., et al., *Generating lineage-specific markers to study Drosophila development.* Dev Genet, 1991. **12**(3): p. 238-52.
6. Rubin, G.M. and A.C. Spradling, *Genetic transformation of Drosophila with transposable element vectors.* Science, 1982. **218**(4570): p. 348-53.
7. Spradling, A.C. and G.M. Rubin, *Transposition of cloned P elements into Drosophila germ line chromosomes.* Science, 1982. **218**(4570): p. 341-7.
8. Venken, K.J. and H.J. Bellen, *Genome-wide manipulations of Drosophila melanogaster with transposons, Flp recombinase, and PhiC31 integrase.* Methods Mol Biol, 2012. **859**: p. 203-28.
9. Venken, K.J. and H.J. Bellen, *Chemical mutagens, transposons, and transgenes to interrogate gene function in Drosophila melanogaster.* Methods, 2014. **68**(1): p. 15-28.
10. Pfeiffer, B.D., et al., *Tools for neuroanatomy and neurogenetics in Drosophila.* Proc Natl Acad Sci U S A, 2008. **105**(28): p. 9715-20.
11. Jenett, A., et al., *A GAL4-driver line resource for Drosophila neurobiology.* Cell Rep, 2012. **2**(4): p. 991-1001.
12. Kvon, E.Z., et al., *Genome-scale functional characterization of Drosophila developmental enhancers in vivo.* Nature, 2014. **512**(7512): p. 91-5.
13. Yanez-Cuna, J.O., et al., *Dissection of thousands of cell type-specific enhancers identifies dinucleotide repeat motifs as general enhancer features.* Genome Res, 2014. **24**(7): p. 1147-56.
14. Tirian, L. and B.J. Dickson, *The VT GAL4, LexA, and split-GAL4 driver line collections for targeted expression in the Drosophila nervous system.* bioRxiv, 2017.
15. Lai, S.L. and T. Lee, *Genetic mosaic with dual binary transcriptional systems in Drosophila.* Nat Neurosci, 2006. **9**(5): p. 703-9.
16. Potter, C.J., et al., *The Q system: a repressible binary system for transgene expression, lineage tracing, and mosaic analysis.* Cell, 2010. **141**(3): p. 536-48.
17. Riabinina, O. and C.J. Potter, *The Q-System: A Versatile Expression System for Drosophila.* Methods Mol Biol, 2016. **1478**: p. 53-78.
18. Feng, K., et al., *Ascending SAG neurons control sexual receptivity of Drosophila females.* Neuron, 2014. **83**(1): p. 135-48.
19. Sen, R., et al., *Moonwalker Descending Neurons Mediate Visually Evoked Retreat in Drosophila.* Curr Biol, 2017. **27**(5): p. 766-771.
20. Ribeiro, I.M.A., et al., *Visual Projection Neurons Mediating Directed Courtship in Drosophila.* Cell, 2018. **174**(3): p. 607-621 e18.
21. Feng, K., et al., *Distributed control of motor circuits for backward walking in Drosophila.* Nat Commun, 2020. **11**(1): p. 6166.
22. Serebreni, L. and A. Stark, *Insights into gene regulation: From regulatory genomic elements to DNA-protein and protein-protein interactions.* Curr Opin Cell Biol, 2021. **70**: p. 58-66.
23. Luan, H., et al., *Refined spatial manipulation of neuronal function by combinatorial restriction of transgene expression.* Neuron, 2006. **52**(3): p. 425-36.
24. Aso, Y., et al., *The neuronal architecture of the mushroom body provides a logic for associative learning.* Elife, 2014. **3**: p. e04577.
25. Aso, Y. and G.M. Rubin, *Dopaminergic neurons write and update memories with cell-type-specific rules.* Elife, 2016. **5**.
26. Wu, M., et al., *Visual projection neurons in the Drosophila lobula link feature detection to distinct behavioral programs.* Elife, 2016. **5**.
27. Robie, A.A., et al., *Mapping the Neural Substrates of Behavior.* Cell, 2017. **170**(2): p. 393-406 e28.

28. Strother, J.A., et al., *The Emergence of Directional Selectivity in the Visual Motion Pathway of Drosophila.* Neuron, 2017. **94**(1): p. 168-182 e10.
29. Dionne, H., et al., *Genetic Reagents for Making Split-GAL4 Lines in Drosophila.* Genetics, 2018. **209**(1): p. 31-35.
30. Namiki, S., et al., *The functional organization of descending sensory-motor pathways in Drosophila.* Elife, 2018. **7**.
31. Wolff, T. and G.M. Rubin, *Neuroarchitecture of the Drosophila central complex: A catalog of nodulus and asymmetrical body neurons and a revision of the protocerebral bridge catalog.* J Comp Neurol, 2018. **526**(16): p. 2585-2611.
32. Dolan, M.J., et al., *Neurogenetic dissection of the Drosophila lateral horn reveals major outputs, diverse behavioural functions, and interactions with the mushroom body.* Elife, 2019. **8**.
33. Davis, F.P., et al., *A genetic, genomic, and computational resource for exploring neural circuit function.* Elife, 2020. **9**.
34. Morimoto, M.M., et al., *Spatial readout of visual looming in the central brain of Drosophila.* Elife, 2020. **9**.
35. Schretter, C.E., et al., *Cell types and neuronal circuitry underlying female aggression in Drosophila.* Elife, 2020. **9**.
36. Turner-Evans, D.B., et al., *The Neuroanatomical Ultrastructure and Function of a Biological Ring Attractor.* Neuron, 2020. **108**(1): p. 145-163 e10.
37. Kind, E., et al., *Synaptic targets of photoreceptors specialized to detect color and skylight polarization in Drosophila.* bioRxiv, 2021.
38. Namiki, S., et al., *A population of descending neurons that regulate the flight motor of Drosophila.* bioRxiv, 2021.
39. Sterne, G.R., et al., *Classification and genetic targeting of cell types in the primary taste and premotor center of the adult Drosophila brain.* Elife, 2021. **10**.
40. Wang, F., et al., *Circuit and Behavioral Mechanisms of Sexual Rejection by Drosophila Females.* Curr Biol, 2020. **30**(19): p. 3749-3760 e3.
41. Wang, F., et al., *Neural circuitry linking mating and egg laying in Drosophila females.* Nature, 2020. **579**(7797): p. 101-105.
42. Wang, K., et al., *Neural circuit mechanisms of sexual receptivity in Drosophila females.* Nature, 2021. **589**(7843): p. 577-581.
43. Golic, K.G. and S. Lindquist, *The FLP recombinase of yeast catalyzes site-specific recombination in the Drosophila genome.* Cell, 1989. **59**(3): p. 499-509.
44. Lis, J.T., J.A. Simon, and C.A. Sutton, *New heat shock puffs and beta-galactosidase activity resulting from transformation of Drosophila with an hsp70-lacZ hybrid gene.* Cell, 1983. **35**(2 Pt 1): p. 403-10.
45. Lee, T. and L. Luo, *Mosaic analysis with a repressible cell marker for studies of gene function in neuronal morphogenesis.* Neuron, 1999. **22**(3): p. 451-61.
46. Xu, T. and G.M. Rubin, *Analysis of genetic mosaics in developing and adult Drosophila tissues.* Development, 1993. **117**(4): p. 1223-37.
47. Isaacman-Beck, J., et al., *SPARC enables genetic manipulation of precise proportions of cells.* Nat Neurosci, 2020. **23**(9): p. 1168-1175.
48. Nern, A., B.D. Pfeiffer, and G.M. Rubin, *Optimized tools for multicolor stochastic labeling reveal diverse stereotyped cell arrangements in the fly visual system.* Proc Natl Acad Sci U S A, 2015. **112**(22): p. E2967-76.
49. Hadjieconomou, D., et al., *Flybow: genetic multicolor cell labeling for neural circuit analysis in Drosophila melanogaster.* Nat Methods, 2011. **8**(3): p. 260-6.
50. Gordon, M.D. and K. Scott, *Motor control in a Drosophila taste circuit.* Neuron, 2009. **61**(3): p. 373-84.
51. McGuire, S.E., et al., *Spatiotemporal rescue of memory dysfunction in Drosophila.* Science, 2003. **302**(5651): p. 1765-8.
52. Nogi, Y., et al., *Interaction of super-repressible and dominant constitutive mutations for the synthesis of galactose pathway enzymes in Saccharomyces cerevisiae.* Mol Gen Genet, 1977. **152**(3): p. 137-44.
53. Lee, T. and L. Luo, *Mosaic analysis with a repressible cell marker (MARCM) for Drosophila neural development.* Trends Neurosci, 2001. **24**(5): p. 251-4.

54. McGuire, S.E., G. Roman, and R.L. Davis, *Gene expression systems in Drosophila: a synthesis of time and space.* Trends Genet, 2004. **20**(8): p. 384-91.
55. Chen, I.W., E. Papagiakoumou, and V. Emiliani, *Towards circuit optogenetics.* Curr Opin Neurobiol, 2018. **50**: p. 179-189.
56. de Mena, L., P. Rizk, and D.E. Rincon-Limas, *Bringing Light to Transcription: The Optogenetics Repertoire.* Front Genet, 2018. **9**: p. 518.
57. Di Ventura, B. and B. Kuhlman, *Go in! Go out! Inducible control of nuclear localization.* Curr Opin Chem Biol, 2016. **34**: p. 62-71.
58. Yamamoto, N. and X.W. Deng, *Protein nucleocytoplasmic transport and its light regulation in plants.* Genes Cells, 1999. **4**(9): p. 489-500.
59. de Mena, L. and D.E. Rincon-Limas, *PhotoGal4: A Versatile Light-Dependent Switch for Spatiotemporal Control of Gene Expression in Drosophila Explants.* iScience, 2020. **23**(7): p. 101308.
60. Chan, Y.B., O.V. Alekseyenko, and E.A. Kravitz, *Optogenetic Control of Gene Expression in Drosophila.* PLoS One, 2015. **10**(9): p. e0138181.
61. Szuts, D. and M. Bienz, *LexA chimeras reveal the function of Drosophila Fos as a context-dependent transcriptional activator.* Proc Natl Acad Sci U S A, 2000. **97**(10): p. 5351-6.
62. Christie, J.M., et al., *Arabidopsis NPH1: a flavoprotein with the properties of a photoreceptor for phototropism.* Science, 1998. **282**(5394): p. 1698-701.
63. Christie, J.M., et al., *LOV (light, oxygen, or voltage) domains of the blue-light photoreceptor phototropin (nph1): binding sites for the chromophore flavin mononucleotide.* Proc Natl Acad Sci U S A, 1999. **96**(15): p. 8779-83.
64. Crosson, S. and K. Moffat, *Photoexcited structure of a plant photoreceptor domain reveals a light-driven molecular switch.* Plant Cell, 2002. **14**(5): p. 1067-75.
65. Horii, T., T. Ogawa, and H. Ogawa, *Nucleotide sequence of the lexA gene of E. coli.* Cell, 1981. **23**(3): p. 689-97.
66. Masuyama, K., et al., *Mapping neural circuits with activity-dependent nuclear import of a transcription factor.* J Neurogenet, 2012. **26**(1): p. 89-102.
67. Rhee, Y., et al., *A genetic system for detection of protein nuclear import and export.* Nat Biotechnol, 2000. **18**(4): p. 433-7.
68. Walker, G.C., *Inducible DNA repair systems.* Annu Rev Biochem, 1985. **54**: p. 425-57.
69. Harper, S.M., L.C. Neil, and K.H. Gardner, *Structural basis of a phototropin light switch.* Science, 2003. **301**(5639): p. 1541-4.
70. Lungu, O.I., et al., *Designing photoswitchable peptides using the AsLOV2 domain.* Chem Biol, 2012. **19**(4): p. 507-17.
71. Zayner, J.P., C. Antoniou, and T.R. Sosnick, *The amino-terminal helix modulates light-activated conformational changes in AsLOV2.* J Mol Biol, 2012. **419**(1-2): p. 61-74.
72. Diensthuber, R.P., et al., *Biophysical, mutational, and functional investigation of the chromophore-binding pocket of light-oxygen-voltage photoreceptors.* ACS Synth Biol, 2014. **3**(11): p. 811-9.
73. Huala, E., et al., *Arabidopsis NPH1: a protein kinase with a putative redox-sensing domain.* Science, 1997. **278**(5346): p. 2120-3.
74. Salomon, M., et al., *Photochemical and mutational analysis of the FMN-binding domains of the plant blue light receptor, phototropin.* Biochemistry, 2000. **39**(31): p. 9401-10.
75. Wang, X., et al., *Light-mediated activation reveals a key role for Rac in collective guidance of cell movement in vivo.* Nat Cell Biol, 2010. **12**(6): p. 591-7.
76. Strickland, D., et al., *TULIPs: tunable, light-controlled interacting protein tags for cell biology.* Nat Methods, 2012. **9**(4): p. 379-84.
77. Niopek, D., et al., *Engineering light-inducible nuclear localization signals for precise spatiotemporal control of protein dynamics in living cells.* Nat Commun, 2014. **5**: p. 4404.
78. Motta-Mena, L.B., et al., *An optogenetic gene expression system with rapid activation and deactivation kinetics.* Nat Chem Biol, 2014. **10**(3): p. 196-202.
79. Guntas, G., et al., *Engineering an improved light-induced dimer (iLID) for controlling the localization and activity of signaling proteins.* Proc Natl Acad Sci U S A, 2015. **112**(1): p. 112-7.
80. Yumerefendi, H., et al., *Control of Protein Activity and Cell Fate Specification via Light-Mediated Nuclear Translocation.* PLoS One, 2015. **10**(6): p. e0128443.

81. Jayaraman, P., et al., *Blue light-mediated transcriptional activation and repression of gene expression in bacteria.* Nucleic Acids Res, 2016. **44**(14): p. 6994-7005.
82. Niopek, D., et al., *Optogenetic control of nuclear protein export.* Nat Commun, 2016. **7**: p. 10624.
83. Kim, M.W., et al., *Time-gated detection of protein-protein interactions with transcriptional readout.* Elife, 2017. **6**.
84. Reade, A., et al., *TAEL: a zebrafish-optimized optogenetic gene expression system with fine spatial and temporal control.* Development, 2017. **144**(2): p. 345-355.
85. Smart, A.D., et al., *Engineering a light-activated caspase-3 for precise ablation of neurons in vivo.* Proc Natl Acad Sci U S A, 2017. **114**(39): p. E8174-E8183.
86. Wang, W., et al., *A light- and calcium-gated transcription factor for imaging and manipulating activated neurons.* Nat Biotechnol, 2017. **35**(9): p. 864-871.
87. Salinas, F., et al., *Fungal Light-Oxygen-Voltage Domains for Optogenetic Control of Gene Expression and Flocculation in Yeast.* mBio, 2018. **9**(4).
88. Zhao, E.M., et al., *Optogenetic regulation of engineered cellular metabolism for microbial chemical production.* Nature, 2018. **555**(7698): p. 683-687.
89. van Haren, J., et al., *Local control of intracellular microtubule dynamics by EB1 photodissociation.* Nat Cell Biol, 2018. **20**(3): p. 252-261.
90. Kim, C.K., et al., *Luciferase-LOV BRET enables versatile and specific transcriptional readout of cellular protein-protein interactions.* Elife, 2019. **8**.
91. Cavanaugh, K.E., et al., *RhoA Mediates Epithelial Cell Shape Changes via Mechanosensitive Endocytosis.* Dev Cell, 2020. **52**(2): p. 152-166 e5.
92. Pfeiffer, B.D., et al., *Refinement of tools for targeted gene expression in Drosophila.* Genetics, 2010. **186**(2): p. 735-55.
93. Loewer, A., et al., *Cell-type-specific processing of the amyloid precursor protein by Presenilin during Drosophila development.* EMBO Rep, 2004. **5**(4): p. 405-11.
94. Emelyanov, A. and S. Parinov, *Mifepristone-inducible LexPR system to drive and control gene expression in transgenic zebrafish.* Dev Biol, 2008. **320**(1): p. 113-21.
95. Nonet, M.L., *Efficient Transgenesis in Caenorhabditis elegans Using Flp Recombinase-Mediated Cassette Exchange.* Genetics, 2020. **215**(4): p. 903-921.
96. Echalier, G., *Drosophila Cells in Culture.* Academic Press, New York. 702 pp., 1997.
97. Velichkova, M., et al., *Drosophila Mtm and class II PI3K coregulate a PI(3)P pool with cortical and endolysosomal functions.* J Cell Biol, 2010. **190**(3): p. 407-25.
98. Shaner, N.C., et al., *Improved monomeric red, orange and yellow fluorescent proteins derived from Discosoma sp. red fluorescent protein.* Nat Biotechnol, 2004. **22**(12): p. 1567-72.
99. Asha, H., et al., *Analysis of Ras-induced overproliferation in Drosophila hemocytes.* Genetics, 2003. **163**(1): p. 203-15.
100. Klapoetke, N.C., et al., *Independent optical excitation of distinct neural populations.* Nat Methods, 2014. **11**(3): p. 338-46.
101. McKellar, C.E., et al., *Threshold-Based Ordering of Sequential Actions during Drosophila Courtship.* Curr Biol, 2019. **29**(3): p. 426-434 e6.
102. Otsuna, H. and K. Ito, *Systematic analysis of the visual projection neurons of Drosophila melanogaster. I. Lobula-specific pathways.* J Comp Neurol, 2006. **497**(6): p. 928-58.
103. Costa, M., et al., *NBLAST: Rapid, Sensitive Comparison of Neuronal Structure and Construction of Neuron Family Databases.* Neuron, 2016. **91**(2): p. 293-311.
104. Panser, K., et al., *Automatic Segmentation of Drosophila Neural Compartments Using GAL4 Expression Data Reveals Novel Visual Pathways.* Curr Biol, 2016. **26**(15): p. 1943-1954.
105. Hindmarsh Sten, T., et al., *Sexual arousal gates visual processing during Drosophila courtship.* Nature, 2021. **595**(7868): p. 549-553.
106. Masse, N.Y., G.C. Turner, and G.S. Jefferis, *Olfactory information processing in Drosophila.* Curr Biol, 2009. **19**(16): p. R700-13.
107. Venken, K.J., et al., *MiMIC: a highly versatile transposon insertion resource for engineering Drosophila melanogaster genes.* Nat Methods, 2011. **8**(9): p. 737-43.
108. Larkin, A., et al., *FlyBase: updates to the Drosophila melanogaster knowledge base.* Nucleic Acids Res, 2021. **49**(D1): p. D899-D907.
109. Jang, A.R., et al., *Drosophila TIM binds importin alpha1, and acts as an adapter to transport PER to the nucleus.* PLoS Genet, 2015. **11**(2): p. e1004974.

110. Gailey, D.A. and J.C. Hall, *Behavior and cytogenetics of fruitless in Drosophila melanogaster: different courtship defects caused by separate, closely linked lesions.* Genetics, 1989. **121**(4): p. 773-85.
111. Stockinger, P., et al., *Neural circuitry that governs Drosophila male courtship behavior.* Cell, 2005. **121**(5): p. 795-807.
112. Cachero, S., et al., *Sexual dimorphism in the fly brain.* Curr Biol, 2010. **20**(18): p. 1589-601.
113. Yu, J.Y., et al., *Cellular organization of the neural circuit that drives Drosophila courtship behavior.* Curr Biol, 2010. **20**(18): p. 1602-14.
114. Bath, D.E., et al., *FlyMAD: rapid thermogenetic control of neuronal activity in freely walking Drosophila.* Nat Methods, 2014. **11**(7): p. 756-62.
115. Inagaki, H.K., et al., *Optogenetic control of Drosophila using a red-shifted channelrhodopsin reveals experience-dependent influences on courtship.* Nat Methods, 2014. **11**(3): p. 325-32.
116. Lu, B., et al., *ppk23-Dependent chemosensory functions contribute to courtship behavior in Drosophila melanogaster.* PLoS Genet, 2012. **8**(3): p. e1002587.
117. Thistle, R., et al., *Contact chemoreceptors mediate male-male repulsion and male-female attraction during Drosophila courtship.* Cell, 2012. **149**(5): p. 1140-51.
118. Toda, H., X. Zhao, and B.J. Dickson, *The Drosophila female aphrodisiac pheromone activates ppk23(+) sensory neurons to elicit male courtship behavior.* Cell Rep, 2012. **1**(6): p. 599-607.
119. Hosokawa, K., et al., *Regional distribution of importin subtype mRNA expression in the nervous system: study of early postnatal and adult mouse.* Neuroscience, 2008. **157**(4): p. 864-77.
120. Kockel, L., et al., *An Interscholastic Network To Generate LexA Enhancer Trap Lines in Drosophila.* G3 (Bethesda), 2019. **9**(7): p. 2097-2106.
121. Kockel, L., et al., *A Drosophila LexA Enhancer-Trap Resource for Developmental Biology and Neuroendocrine Research.* G3 (Bethesda), 2016. **6**(10): p. 3017-3026.
122. Fischbach, K.-F. and A.P.M. Dittrich, *The optic lobe of Drosophila melanogaster. I. A Golgi analysis of wild-type structure.* Cell Tissue Res, 1989. **258**: p. 441-475.
123. Huberman, A.D., M.B. Feller, and B. Chapman, *Mechanisms underlying development of visual maps and receptive fields.* Annu Rev Neurosci, 2008. **31**: p. 479-509.
124. Nassi, J.J. and E.M. Callaway, *Parallel processing strategies of the primate visual system.* Nat Rev Neurosci, 2009. **10**(5): p. 360-72.
125. Petersen, C.C.H., *Sensorimotor processing in the rodent barrel cortex.* Nat Rev Neurosci, 2019. **20**(9): p. 533-546.
126. Montell, C., *Drosophila visual transduction.* Trends Neurosci, 2012. **35**(6): p. 356-63.
127. Kim, S.S., et al., *Ring attractor dynamics in the Drosophila central brain.* Science, 2017. **356**(6340): p. 849-853.
128. Gibson, D.G., et al., *Enzymatic assembly of DNA molecules up to several hundred kilobases.* Nat Methods, 2009. **6**(5): p. 343-5.
129. McQuin, C., et al., *CellProfiler 3.0: Next-generation image processing for biology.* PLoS Biol, 2018. **16**(7): p. e2005970.
130. Schindelin, J., et al., *Fiji: an open-source platform for biological-image analysis.* Nat Methods, 2012. **9**(7): p. 676-82.